V.YA. DEGODA,[1] M.S. BRODYN,[2] M. ALIZADEH,[1] G.P. PODUST,[1] N.YU. PAVLOVA,[3] B.V. KOZHUSHKO[2]

[1] Taras Shevchenko National University of Kyiv, Faculty of Physics
 (4, Akademika Glushkova Ave., Kyiv 03127, Ukraine)
[2] Institute of Physics, Nat. Acad. of Sci. of Ukraine
 (46, Nauky Ave., Kyiv 03028, Ukraine)
[3] Dragomanov National Pedagogical University
 (9, Pyrogova Str., Kyiv 01601, Ukraine)

DIPOLE-CENTER IN ZnSe CRYSTALS

It has been found that the well-known luminescence band with a maximum near 630 nm in undoped ZnSe crystals is associated with the recombination of free electrons at localized holes and free holes at localized electrons. The result was achieved by comparing experimental values for the stationary luminescence intensity with the phosphorescence and thermally stimulated luminescence intensities, as well as values obtained for the conductivity under stationary conditions with curves registered for the relaxation current and the thermally stimulated conductivity. For the explanation of uncharacteristic spectral features of the luminescence band at about 630 nm, the existence of a complex (nonlocalized) center has been proposed, with a possibility for both recombination mechanisms to be realized at it. We propose to call it "dipole-center". A theoretical analysis is performed for the multicenter model of crystal phosphor with a recombination dipole-center. It is shown that just the presence of the dipole-center gives rise to the appearance of a wide luminescence band with a general maximum at 630 nm. This fact allows a scintillation material of the new type to be proposed, where the dipole-center plays the role of a luminescence center that does not demand traps for a high luminescence yield.

K e y w o r d s: ZnSe, luminescence centers in crystal phosphors, luminescence, dipole-center.

1. Introduction

Zinc selenide (ZnSe) belongs to wide-band semiconductors $A^{II}B^{VI}$ [1–8] and has been studied for a long time. ZnSe crystals are a good model material for studying the physical processes of luminescence and conductivity kinetics in high energy-gap semiconductors excited with UV and X-ray quanta. They are also used to create semiconductor electronic devices and information display systems. Another promising area of ZnSe application as detectors of ionizing radiation with indirect [4–7] and direct [8] conversion

of the fluxes of high-energy quantum and particles into electric current was developed during the last decade. Nowadays, the combination of the electrophysical, physicochemical, and luminescence properties of zinc selenide doped with tellurium [ZnSe(Te)], as well as its radiation resistance, makes it one of the most effective scintillators for the application in detectors of the scintillator–photodiode type [5–7], where a wide luminescence band with a maximum at 630 nm is used.

The application of specially undoped ZnSe as a semiconductor detector became possible only after the development of technologies for growing high-quality single crystals with low concentrations of uncontrolled impurities and high resistivity of the mate-

rial at a level of 10^{10}–10^{14} $\Omega \cdot$cm. It should be noted that the relatively high value of the effective atomic number $Z_{\text{eff}} = 32$ and the wide band gap $E_g = 2.7$ eV (at 300 K) make zinc selenide a promising material for X-ray detectors without cooling [8]. The semiconductor detectors of this type work well under irradiation in the dc registration mode, but only some specimens allow the detection of current pulses. It occurs owing to the presence of a noticeable concentration of traps in ZnSe crystals, which reduce the amplitude of the current pulse and stretch it in time, i.e., increase its duration [9].

The recombination band in ZnSe with a maximum at 630 nm is known to possess some specific features. For instance, the spectral position of the maximum varies from 615 to 645 nm in various specimens. Therefore, a conclusion was drawn that this band is complex and consists of at least two elementary bands, with the spectral distance between them being less than the half-widths of the elementary components. Furthermore, when comparing the following quantities with one another after prolonged X-ray excitation of the specimens at 85 K [10]:

1. the stationary luminescence intensities of the 630- and 970-nm bands (J_{XRL}) and the stationary X-ray conductivity current (i_{XRC});

2. the phosphorescence intensities (at time moments of 50, 150, and 300 s) in the 630- and 970-nm bands (J_{Ph}) and the conductivity relaxation current at time moments of 50, 150, and 300 s after excitation (i_{RC});

3. the intensities of thermally stimulated luminescence (at temperatures of 110, 130, and 150 K) in the 630- and 970-nm bands (J_{TSL}) and the current of thermally stimulated conductivity (at temperatures of 110, 130, and 150 K) (i_{TSC}).

It was found that the stationary intensity of the 630-nm band at 85 K is a few tens times higher than the expected one. It can be demonstrated as follows. The following ratios:

for the conduction current,

$$V_{\text{XRC}} : i_{\text{RC}} \begin{pmatrix} 50 \text{ s} \\ 150 \text{ s} \\ 300 \text{ s} \end{pmatrix} : i_{\text{TSC}} \begin{pmatrix} 110 \text{ K} \\ 130 \text{ K} \\ 150 \text{ K} \end{pmatrix};$$

for the intensity of luminescence band at 970 nm,

$$J_{\text{XRL}} : J_{\text{Ph}} \begin{pmatrix} 50 \text{ s} \\ 150 \text{ s} \\ 300 \text{ s} \end{pmatrix} : J_{\text{TSL}} \begin{pmatrix} 110 \text{ K} \\ 130 \text{ K} \\ 150 \text{ K} \end{pmatrix};$$

for the intensity of luminescence band at 630 nm,

$$C \cdot J_{\text{XRL}} : J_{\text{Ph}} \begin{pmatrix} 50 \text{ s} \\ 150 \text{ s} \\ 300 \text{ s} \end{pmatrix} : J_{\text{TSL}} \begin{pmatrix} 110 \text{ K} \\ 130 \text{ K} \\ 150 \text{ K} \end{pmatrix};$$

are identical if the constant C for the X-ray intensity of the 630-nm band is much less than unity. In those ratios, only one value stands out, this is the intensity of the stationary luminescence of the 630-nm band. It occurs because the 630-nm luminescence band is in the X-ray luminescence spectrum but not in the phosphorescence and thermally stimulated luminescence spectra, which can be explained only if we suppose that the luminescence of either of two elementary bands at 630 nm takes place following the hole recombination mechanism (i.e., the recombination of a free hole with an electron located at the luminescence center). Accordingly, this elementary band is absent in the phosphorescence processes and in the thermally stimulated luminescence ones. The other elementary band at 630 nm and the band at 970 nm are associated with the electron mechanism of recombination (i.e., the recombination of a free electron with a hole located at the luminescence center). At the same time, the X-ray conductivity current, the conductivity current relaxation, and the thermally stimulated conductivity are governed by free electrons. This scenario agrees with the results obtained in work [3], where it was found that the photoconductivity current in ZnSe crystals is created by free electrons.

In work [11], a model was proposed for a luminescence center at which both alternative recombination mechanisms can be realized, the dipole-center model. Centers with a dipole moment were reported earlier [12–16], but they were not considered as luminescence centers. Besides the creation of a complex dipole defect, the dipole-center can also be realized as a limiting case of a donor-acceptor pair created at room temperature from deep donor and acceptor impurities located in neighbor sites of the crystal lattice.

The authors of work [17] pointed out that radiation emission by various defects in zinc selenide can be observed in this spectral interval. In particular, the band can be emitted by a c-band–acceptor radiative transition in the donor-acceptor pair $\{V_{\text{Zn}}-D^+\}^0$ or $\{V_{\text{Zn}}-Te_{\text{Se}}^0-D^+\}^0$. In work [18], it was proposed that in the case of ZnSe nanowires, the band near 635 nm is associated with the recombination in the donor-acceptor pair, where the acceptor is V_{Zn} and

the donor is V_{Se} or Zn_i. A team of researchers [19–24] proposed the following structure for the center in ZnSe crystals which is responsible for the 630-nm luminescence band: this is a complex defect consisting of an isoelectronic selenium impurity, in particular, an oxygen or tellurium ion located near the zinc vacancy.

This work was not aimed at establishing the chemical nature of the indicated luminescence center because we do not have enough experimental information. We tried to make sure that from the physical point of view, this center, which is responsible for the luminescence band at 630 nm, is a dipole at which both electrons and holes can be localized, and luminescence occurs at the localization of the opposite-sign charge carrier. For this purpose, the following tasks had to be fulfilled:

1. to carry out a comprehensive analysis of experimental spectroscopic results for the 630-nm luminescence band, given in the literature and ours, to obtain an answer to the question: Is this a single center where both recombination mechanisms are implemented, or do we deal with two independent centers? and to determine an appropriate experimental verification of this assumption;

2. to explain the experimental luminescence features for the luminescence band with a maximum at 630 nm in ZnSe crystals.

2. Experimental Technique

Zinc selenide (ZnSe) crystals were grown from a pre-purified charge. They were not specially doped during their growth. As a result, specimens with a minimum concentration of point defects and a maximum resistivity ($\rho \sim 10^{12} \div 10^{14} \ \Omega \cdot cm$) were obtained. For research, specimens $18 \times 9 \times 2 \ mm^3$ in size were cut out from various crystal boules and polished.

Complex experimental studies of photo- (PC) and X-ray conductivity (XRC), photo- (PL) and X-ray luminescence (XRL), phosphorescence (Ph), conductivity current relaxation (RC), thermally stimulated conductivity (TSC), and thermally stimulated luminescence (TSL) were performed.

To study conductivity, three-layer metal electrical contacts in the form of two parallel strips ($1 \times 5 \ mm^2$) were sputtered on single crystals using the resistive method, and copper conductors were soldered to them. The distance d between the electrodes was 5 mm. One electrode was supplied with a stabilized voltage ranging from 0 to 1000 V, and the other was connected to a nanoammeter. The latter allowed the current to be measured with an accuracy of ± 1 pA if the current did not exceed 100 pA, and with an accuracy of 1% for higher currents. For all conduction current values, the input impedance of the nanoammeter was several orders of magnitude lower than the electrical resistance of the ZnSe specimen.

X-ray excitation (X-excitation) of ZnSe specimens was performed by means of integral radiation from an X-ray tube BHV-7 (Re, 20 kV, 5–25 mA, the anode of the tube was at a distance of 130 mm from the specimen) through a beryllium window of cryostat. A specific feature of such X-excitation is the lack of generation of new radiation-induced defects so that only recharging of existing defects in the crystal is possible. For photoexcitation (UV-excitation), we used seven ultraviolet LEDs of the UF-301 type with a maximum radiation emission at 395 nm, i.e., the energy of UV quanta was higher than the width of the ZnSe band gap. All seven LEDs were arranged on the same mounting panel with the width $W = 20$ mm, and they had a common power supply that allowed the magnitude of stabilized current through the LEDs to be varied within an interval of 30–180 mA. The radiation emission of each LED from a distance of 55 mm was directed through the quartz window of cryostat toward the test specimen. Preliminary it was experimentally found that the shape of the emission spectrum of LEDs did not depend on the magnitude of the current through them. A semiconductor laser with a power of 350 mW at $\lambda = 532$ nm was used for intracenter excitation of the luminescence centers responsible for the 630-nm band.

The specimen luminescence was registered via two independent channels: integrally through an optical light filter (OS-13) and spectrally through a large-aperture monochromator MDR-2 ($S_p = 8$ nm) at various wavelengths. Simultaneously, the current flowing through the single-crystalline ZnSe specimen was measured. After the excitation termination, phosphorescence and conduction current relaxation were measured during 5–10 min. Then, the specimen was heated up and the TSL and TSC curves were measured. In both cases, the heating rate was about 0.30 K/s. Luminescence and conductivity were studied in vacuum (<1 Pa). All luminescence spectra were corrected for the spectral sensitivity of the registration system.

3. Spectral Characteristics of Luminescence in ZnSe Crystals

The PL and XRL spectra of zinc selenide crystals have already been studied at length [1, 4, 5, 7, 24, 25]. Various specimens demonstrate edge luminescence (recombination of excitons at shallow centers), luminescence of donor-acceptor pairs (DAPs), and various luminescence bands in the visible and infrared spectral intervals. In specially undoped high-resistance ZnSe crystals, two wide bands with maxima near 630 and 970 nm are usually observed at temperatures from 8 to 400 K. The 630-nm luminescence band is of special interest because it is known that this band is not elementary and its two constituent elementary subbands are generated by opposite recombination mechanisms. As a result, different spectral positions of the total maximum are observed at different component ratios. Figure 1 illustrates the XRL spectra of the 630-nm band for seven various ZnSe samples. One can see that the intensity of this band differs for different samples, and the spectral positions of the maximum are also different. It was also observed that some specimens demonstrate weak edge luminescence (Fig. 2). No other luminescence bands were observed in undoped high-resistance ZnSe crystals. The presence of the elementary luminescence band at 970 nm, the intensity of which varies for various specimens (Fig. 2), considerably facilitates the analysis of spectral characteristics because it allows comparing the 630- and 970-nm bands. Both of those luminescence bands are recombination by nature because they are observed in both the phosphorescence and thermally stimulated luminescence spectra [10].

It was found [25] that the shapes of the indicated luminescence bands, the spectral positions of their maxima, and even the ratios of luminescence band intensities do not change if the intensities of UV- and X-excitations vary at various temperatures (8– 420 K). A comparison of the PL and XRL spectra [11] shows that the spectral positions of the 630-nm band maxima are most different at room temperature. This fact allowed the band at 630 nm, using the Alentsev–Fok method [26], to be resolved into elementary components [27], which are well described by Gaussians [28] with the half-width δ:

$$J\left(h\nu\right)_{\text{lum}} = J_0 \exp\left[-\left(2\ln 2\right)^2 \frac{\left(h\nu - h\nu_0\right)^2}{\delta^2}\right]. \quad (1)$$
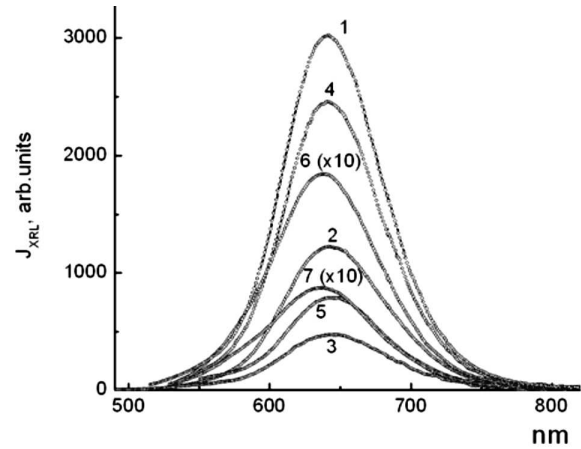

Fig. 1. XRL spectra of the 630-nm band in seven ZnSe specimens at a temperature of 85 K
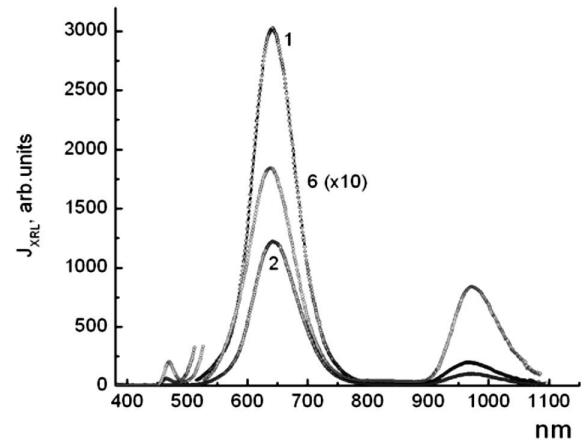

Fig. 2. General XRL spectra of three ZnSe specimens at 85 K (the curve numeration as in Fig. 1)

In addition, a comparison of the temperature dependences of the short- and long-wave components of the 630-nm band with the temperature dependences of the 970-nm band (the electron recombination mechanism) and the conductivity (induced by free electrons) made it possible to establish the recombination mechanisms of elementary components:

• D^+-band at 1.875 eV (661 nm), $\delta = 0.181$ eV (the hole recombination mechanism);

• D^--band at 2.028 eV (611 nm), $\delta = 0.196$ eV (the electron recombination mechanism).

The difference between the positions of the maxima of the elementary bands is less than the half-width of each band and therefore their sum produces a single total maximum. It was verified that for other ZnSe
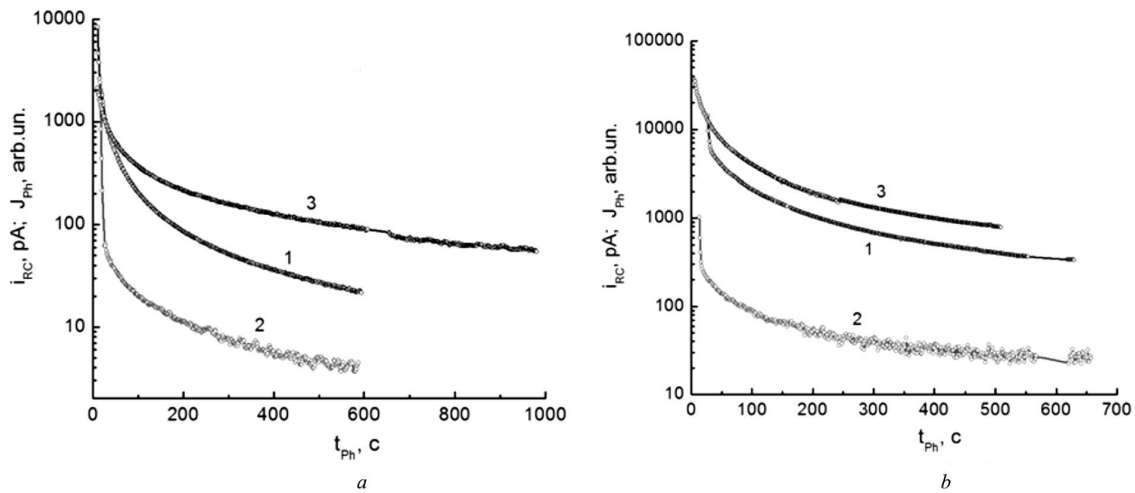
Fig. 3. Dependences of phosphorescence quenching in the 630-nm (*1*) and 970-nm (*2*) bands and conductivity current relaxation (*3*) after UV- (*a*) and X-excitation (*b*) of the ZnSe specimen at a temperature of 8 K ($U_0 = 3.2$ V)

samples, the 630-nm band in the XRL and PL spectra obtained at room temperature is also resolved into the same components. This fact confirms the unambiguity of the resolution into elementary components. It is various intensity ratios of elementary components that determine the spectral position of the 630-nm band in various ZnSe specimen.

A detailed study of lux-luminescence characteristics (the dependence of the luminescence intensity on the excitation intensity) at various temperatures [29] showed that they are almost linear and similar for the 630- and 970-nm bands in the XRL and PL spectra. The lux-luminescence characteristics of those bands are also similar in shape to the lux-ampere characteristics of conductivity [30]. This means that if the intensities of UV- and X-excitations changes at a fixed temperature (within the temperature interval from 8 to 420 K), the basic processes, starting from the generation of free charge carriers to their recombination with emission of light quanta, do not change.

In ZnSe crystals, phosphorescence (J_{Ph}) in both 630- and 970-nm luminescence bands and relaxation of conductivity current (i_{RC}) are observed at a temperature of 85 K after UV- and X-excitations [10]. Moreover, at 85 K, the spectral composition of phosphorescence practically coincides with the XRL spectrum of this band. Phosphorescence and conductivity current relaxation are also observed at 8 K. In Fig. 3, the phosphorescence (Ph) and current relaxation (RC) curves are depicted, which were registered at 8 K in the 630- and 970-nm bands under the exci-

tation of two types. Phosphorescence in different luminescence bands was registered using different photoelectronic multipliers and at various sensitivities of registration system, only in order to ensure that they are similar. From Fig. 3, when comparing the phosphorescence quenching curves and the conductivity current relaxation curves, one can see that the formers are driven by the mechanism of recombination of thermally delocalized electrons from traps.

Thus, the light sum accumulated in the specimen under excitation manifests itself in the form of phosphorescence and conductivity current relaxation. At the further heating of the specimen, the light sum accumulated at deep traps manifests itself in the form of thermoactivation processes, which are registered in TSL and TSC. The TSL curves in the 630-nm [$J_{\mathrm{TSL}}(630)$] and 970-nm [$J_{\mathrm{TSL}}(970)$] bands and the TSC curves (i_{TSC}) were registered simultaneously. In all cases, there appeared the same peaks, although their intensities could be several times different in various specimens. It should also be noted that the TSL peaks in ZnSe crystals have a larger half-width than in many oxide crystals (for example, $\delta \approx 20$ K for the peak $T_m = 183$ K), which brings about the overlapping of neighbor peaks. In Fig. 4, the TSL and TSC curves after X-excitation (for 1 h) at temperatures of 8 and 85 K are exhibited. The application of two or three (additionally, at 295 K) excitation temperatures allows the registration of all main peaks because the cross-sections of free electron localization depend on the trap depth and the excitation temperature.
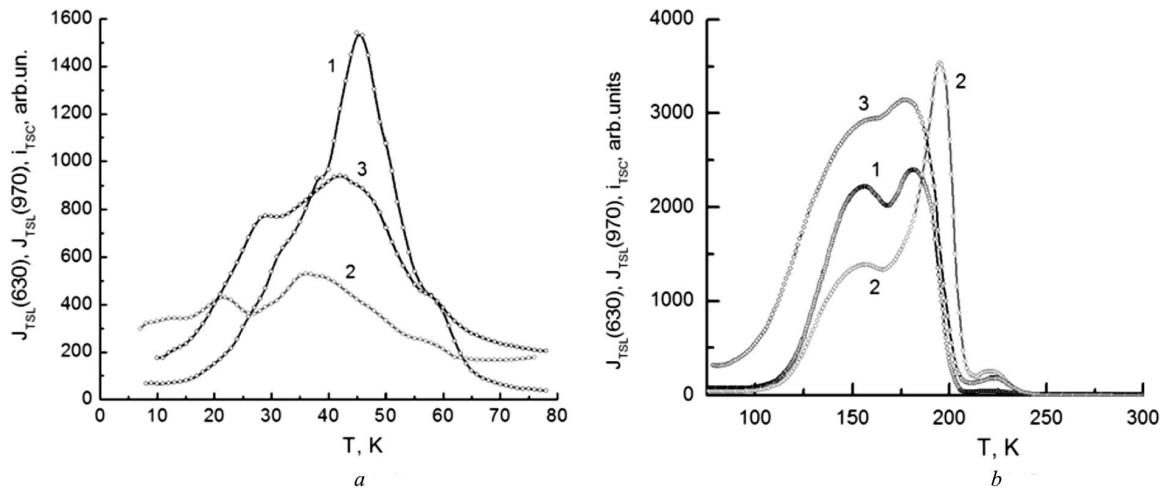
Fig. 4. Temperature dependences of $J_{\text{TSL}}(630)$ (*1*), $J_{\text{TSL}}(970)$ (*2*), and i_{TSC} (*3*) obtained after X-ray excitation of a ZnSe specimen for 1 h at 8 K (*a*) and 85 K (*b*)

A comparison was made between the intensities of TSL peaks and the intensities of PL and XRL bands for various ZnSe samples. No correlations were found.

Thus, prolonged phosphorescence in the 630- and 970-nm bands and conductivity current relaxation are observed in ZnSe single crystals, as well as TSL and TSC at specimen heating. This testifies to the recombination nature of luminescence at those recombination centers when free *e-h* pairs are generated.

4. Schemes of Electronic Transitions at Excitation at Luminescence Centers

A simple physical model of recombination center is required which could explain a possibility of alternative implementation of both recombination mechanisms. In turn, this means that such a center in the initial state can be a trap for both free electrons and free holes. The dipole-center model has been proposed as such a center [11]. The dipole-center is not a point defect but a complex of at least two different defects that possess opposite local charges and create a stationary complex dipole-center. By its characteristics, such a center is close to the donor-acceptor pair, in which the donor and acceptor are located at the neighbor sites in the crystal lattice. Such a center must provide spatial and charge compensation, but one of its parts has an additional positive charge, and the other an additional negative charge. This means that with respect to charges, such a complex is a dipole. Additional negative and positive charges do not have to be identical. A characteristic feature of such a recombination center is its ability to localize a free electron in its environment near the positive charge of the dipole-center or localize a free hole near the negative charge. A subsequent localization of a carrier with the opposite charge sign leads to their recombination and emission of a light quantum.

The application of the band structure of semiconductors in the kinetic theory of PL [31], [32] and PC [33–35] makes it possible to present the schemes of electronic transitions and obtain the systems of kinetic equations. The absorption of quanta with energies higher than the band gap width ($h\nu > E_g$) is known to generate free electrons in the conduction band and free holes in the valence band, and recombination of those free *e-h* pairs at luminescence centers gives rise to recombination luminescence. The electron mechanism of recombination is illustrated in Fig. 5, where the main and excited energy levels of a luminescence center are depicted schematically. The electron mechanism of recombination (Fig. 5) is realized in four stages: first, a hole is localized at the center (the center recharging); then, an electron localization takes place, which is accompanied by the energy transfer from the electron-hole pair to the center; afterward, the center transits into an excited state, which spontaneously transforms into the ground state with the emission of a light quantum.

The scheme of the hole mechanism of recombination is shown in Fig. 6. In addition to the levels of the luminescence center, the level of the electron
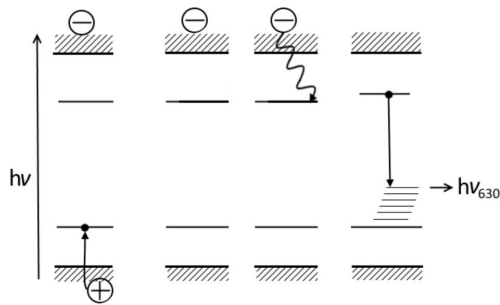
Fig. 5. Electronic transitions in the electron mechanism of recombination
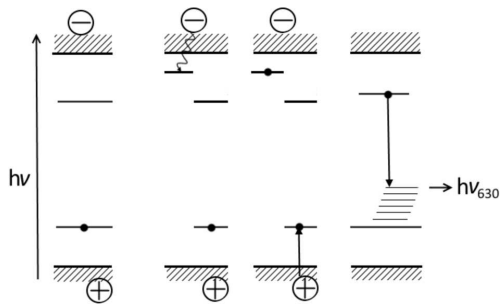

Fig. 6. Electronic transitions in the hole mechanism of recombination

trap is also shown schematically. The hole mechanism of recombination (Fig. 6) also has four stages: first, an electron is localized at the center (the center recharging); then, the hole localization takes place, which is accompanied by the energy transfer from the electron-hole pair to the center; then, the latter transits into an excited state, which spontaneously transforms into the ground state with the emission of a light quantum.

If there is a charge carrier near the dipole-center or in its nearest vicinity, then spatial shifts of the components of the complex defect should take place, and they will be different for the electron and hole localizations. If a free carrier of the opposite sign is localized, we obtain different initial spatial configurations of the excited luminescence center. As a result, we will have slight differences between the luminescence spectra given by different recombination mechanisms.

When considering the luminescence kinetics, it is also necessary to take into account that a free electron can be localized at any trap (shallow, phosphorescence, deep). A free hole in the valence band can recombine with the electron localized at the trap, but it usually results in nonradiative recombination.

5. Calculation of the Intensity Ratio for the Luminescence D^-- and D^+-Bands

The required theoretical calculations will be carried out for the multi-center model of crystal phosphor [36], which is closest to the wide-band-gap ZnSe crystals. Unlike the classical crystal phosphor model [31, 32], the multi-center crystal model contains three types of electron traps (shallow, phosphorescence, and deep ones) and several recombination centers with the electron and hole recombination mechanisms. Moreover, a hole can be localized at a recombination center with the electron recombination mechanism in the uncharged state, i.e., it can be a deep trap for holes. At the same time, an electron can be localized at a recombination center with the hole recombination mechanism in the uncharged state, i.e., such a center is a deep trap for electrons.

To determine the origin of the 630-nm luminescence band in ZnSe, two models can be used: (i) there are two independent centers with opposite recombination mechanisms and close luminescence spectra and (ii) there is only one dipole-center (the luminescence spectra should be close to each other). Therefore, those two models have to be considered theoretically and an experimental criterion determining which model is correct for ZnSe crystals has to be found.

5.1. Model of crystal phosphor with different recombination centers

The first model of crystal phosphor contains two independent types of luminescence centers with either the electron or the hole recombination mechanism. The concentrations of the luminescence centers are v_{n_1} and v_{p_1}, respectively. Their luminescence bands are spectrally close, and the corresponding maxima are located near a wavelength of 630 nm. Under excitation, electrons and holes are localized at those centers, with their concentrations being n_1 and p_1, respectively. Recharged recombination centers are formed at that. Let us assume that free electrons can be localized at deep traps, the concentration of which is v_d, and the corresponding concentration of localized electrons is n_d. We also assume that the material also contains recombination centers with luminescence in the IR interval (at about 970 nm), at which the electron mechanism of recombination is realized. The concentration of IR centers is v_{p_2}, and the corresponding concentration of localized holes is p_2.

For this model, a system of differential kinetic equations can be written where each equation describes one of possible states for charge carriers [36]. Note that the localization processes of free electrons at traps and free holes at recombination centers are similar and can be described by similar terms in the differential equations. Under long permanent excitation, the system transits into a stationary quasi-equilibrium state in which all time derivatives become equal to zero. Then, the system of kinetic equations transforms into the following system of algebraic equations:

$$
\begin{cases}
N^- = G\tau^-, \\
P^+ = G\tau^+, \\
0 = N^- u^- \sigma_d^- \left(v_d - n_d\right) - P^+ u^+ \sigma_d^+ n_d, \\
0 = N^- u^- \sigma_{n_1}^- \left(v_{n_1} - n_1\right) - P^+ u^+ \sigma_{n_1}^+ n_1, \\
0 = P^+ u^+ \sigma_{p_1}^+ \left(v_{p_1} - p_1\right) - N^- u^- \sigma_{p_1}^- p_1, \\
0 = P^+ u^+ \sigma_{p_2}^+ \left(v_{p_2} - p_2\right) - N^- u^- \sigma_{p_2}^- p_2, \\
N^- + n_d + n_1 = P^+ + p_1 + p_2,
\end{cases}
\tag{2}
$$

where N^- and P^+ are the concentrations of free electrons and holes, respectively; G is the generation rate of pairs from free charge carriers per unit volume per unit time; τ^- and τ^+ are the lifetimes of free electrons and holes, respectively, in the bands; u^- and u^+ are the thermal velocities of free electrons and holes, respectively; $\sigma_c^{+/-}$ are the cross-sections of localization and recombination for free electrons and holes (the superscript indicates the free carrier charge, and the subscript the center at which this carrier is localized). The last equation in system (2) is conventionally called the balance equation. Its necessity is dictated by the law of charge conservation.

We will use assumptions adopted in the classical theories of photoluminescence and photoconductivity [31–35] and confirmed by plenty of experimental results. They substantially facilitate the obtaining of the solutions for system (2). In particular, the concentrations of free charge carriers are taken to be much lower than the concentrations of localized carriers, $(N^-, P^+) \ll (n_d, n_1, p_1, p_2)$, which makes the balance equation much simpler. Although all cross-sections are different, they can be united into two groups: localization cross-sections σ_{loc} ($\sigma_d^- \approx \sigma_{n_1}^- \approx$ $\approx \sigma_{p_1}^+ \approx \sigma_{p_2}^+ \approx \sigma_{\text{loc}}$) and recombination cross-sections σ_{rec} ($\sigma_d^+ \approx \sigma_{n_1}^+ \approx \sigma_{p_1}^- \approx \sigma_{p_2}^- \approx \sigma_{\text{rec}}$). In the first case, the charge carrier is localized at a center with a small

additional charge; in the second one, at an already oppositely recharged center. These simplifications are based on the fact that all cross-sections of electron localization at traps in ZnSe are different within an order of magnitude [37]. Additionally, from the studies of the X-ray conductivity current actuation in ZnSe crystals [38], it was found that the cross-sections of electron localization at traps and recombination centers also differ within an order of magnitude. Such assumptions considerably simplify calculations without changing the physical result.

In all kinetic equations, the probability of free electron localization at a center is determined by the product of the electron localization cross-section and the concentration of this center, $\sigma_i v_i$. The localization cross-section is a parameter of the center, i.e., a constant value, whereas the concentration of the centers can vary by orders of magnitude in various specimens. Therefore, actually, we make the substitution $\sigma_i v_i = \sigma_{\text{loc}} v_i (\sigma_i / \sigma_{\text{loc}}) = \sigma_{\text{loc}} v_i^*$, where $v_i^* = v_i \sigma_i / \sigma_{\text{loc}}$ is the effective concentration of the centers, which is slightly different from the actual concentration and which will be used in further mathematical calculations. It is also clear that $\sigma_{\text{loc}} < \sigma_{\text{rec}}$, so we introduce the dimensionless parameter $\delta = \sigma_{\text{rec}} / \sigma_{\text{loc}}$, and we will change it within an order of magnitude. In this model, shallow traps are neglected because a small number of electrons are localized at them so that they do not affect the stationary concentrations of recharged deep traps and recombination centers, as well as recombination fluxes in the stationary state of crystal phosphor.

As the intensity of recombination luminescence J, we will call the number of recombination acts at the center per unit volume per unit time. The intensities are proportional to the experimentally registered luminescence intensities of the bands. Thus, according to Eq. (2), for the components of the luminescence band intensity, we can write:

• the component

$$
J_{n_r}^+ = N^- u^- \sigma_{\text{loc}} \left(v_d - n_d\right) = P^+ u^+ \sigma_{\text{rec}} n_d
$$

is associated with non-radiative recombination of free holes with trapped electrons (this component was not experimentally registered at all temperatures);

• the component

$$
J_{n_1}^+ = N^- u^- \sigma_{\text{loc}} \left(v_{n_1} - n_1\right) = P^+ u^+ \sigma_{\text{rec}} n_1
$$

is associated with recombination of free holes at the 630-nm center according to the hole recombination mechanism;

• the component

$$J_{p_1}^- = P^+ u^+ \sigma_{\text{loc}} (v_{p_1} - p_1) = N^- u^- \sigma_{\text{rec}} p_1$$

is associated with recombination of free electrons at the 630-nm center according to the electron recombination mechanism;

• and the component

$$J_{p_2}^- = P^+ u^+ \sigma_{\text{loc}} (v_{p_2} - p_2) = N^- u^- \sigma_{\text{rec}} p_2$$

is associated with recombination of free electrons at the 970-nm center according to the electron recombination mechanism.

Let us apply the dimensionless parameter $a_1 = N^- u^- / P^+ u^+ = \tau^- u^- / \tau^+ u^+$ in order to express the concentrations of localized charge carriers via the concentrations of the centers and the parameters δ and a_1:

$$n_d = v_d \frac{N^- u^- \sigma_{\text{loc}}}{N^- u^- \sigma_{\text{loc}} + P^+ u^+ \sigma_{\text{rec}}} = \frac{v_d}{1 + \frac{\delta}{a_1}} = v_d r_e, \tag{3a}$$

$$n_1 = v_{n_1} \frac{N^- u^- \sigma_{\text{loc}}}{N^- u^- \sigma_{\text{loc}} + P^+ u^+ \sigma_{\text{rec}}} = \frac{v_{n_1}}{1 + \frac{\delta}{a_1}} = v_{n_1} r_e, \tag{3b}$$

$$p_1 = v_{p_1} \frac{P^+ u^+ \sigma_{\text{loc}}}{N^- u^- \sigma_{\text{loc}} + P^+ u^+ \sigma_{\text{rec}}} = \frac{v_{p_1}}{1 + a_1 \delta} = v_{p_1} r_h, \tag{3c}$$

$$p_2 = v_{p_2} \frac{P^+ u^+ \sigma_{\text{loc}}}{N^- u^- \sigma_{\text{loc}} + P^+ u^+ \sigma_{\text{rec}}} = \frac{v_{p_2}}{1 + a_1 \delta} = v_{p_2} r_h, \tag{3d}$$

$$\frac{n_d}{v_d} = \frac{n_1}{v_{n_1}} = \frac{1}{1 + \frac{\delta}{a_1}} = r_e, \tag{3e}$$

$$\frac{p_1}{v_{p_1}} = \frac{p_2}{v_{p_2}} = \frac{1}{1 + a_1 \delta} = r_h. \tag{3f}$$

The recharging levels of electron (r_e) and hole (r_h) centers are identical. For the accumulated light sum Σ_1, we may write

$$\Sigma_1 = (p_1 + p_2) = \frac{(v_{p_1} + v_{p_2})}{1 + a_1 \delta} = $$
$$= (n_i + n_1) = \frac{(v_i + v_{n_1}) a_1}{a_1 + \delta}$$

so that

$$\frac{v_{p_1} + v_{p_2}}{v_i + v_{n_1}} = a_1 \left(\frac{1 + a_1 \delta}{a_1 + \delta} \right).$$

The same conclusion was obtained earlier [36] for a simpler model of crystal phosphor. This conclusion testifies that from the physical point of view, further addition of any other similar centers to the model will not lead to principally different results. In the framework of the model concerned, the recharging levels of the electron and hole centers are

$$r_e = \frac{(v_{p_1} + v_{p_2})}{(v_{p_1} + v_{p_2}) + (v_d + v_{n_1})}$$

and

$$r_h = \frac{(v_d + v_{n_1})}{(v_{p_1} + v_{p_2}) + (v_d + v_{n_1})}.$$

Substituting the obtained relationships for concentrations (3) into the balance equation and taking into account that

$$\frac{v_d}{1 + \frac{\delta}{a_1}} + \frac{v_{n_1}}{1 + \frac{\delta}{a_1}} = \frac{v_{p_1}}{1 + a_1 \delta} + \frac{v_{p_2}}{1 + a_1 \delta}$$

so that

$$\frac{v_d + v_{n_1}}{1 + \frac{\delta}{a_1}} = \frac{v_{p_1} + v_{p_2}}{1 + a_1 \delta},$$

we obtain the following quadratic equation for the dimensionless parameter a_1:

$$a_1^2 - \frac{a_1}{\delta} \left[\left(\frac{v_{p_1} + v_{p_2}}{v_d + v_{n_1}} \right) - 1 \right] - \left(\frac{v_{p_1} + v_{p_2}}{v_d + v_{n_1}} \right) = 0. \tag{4}$$

By its nature, the parameter a_1 cannot be negative. Therefore, the dependence of a_1 on the concentrations of the centers and the ratio between the recombination and localization cross-sections looks like

$$a_1 = \frac{1}{2\delta} \left[\left(\frac{v_{p_1} + v_{p_2}}{v_d + v_{n_1}} \right) - 1 \right] + $$

$$+ \sqrt{ \frac{1}{4\delta^2} \left[\left(\frac{v_{p_1} + v_{p_2}}{v_d + v_{n_1}} \right) - 1 \right]^2 + \left(\frac{v_{p_1} + v_{p_2}}{v_d + v_{n_1}} \right)}. \tag{5}$$

In Fig. 7, the dependences of a_1 on the ratio between the total concentrations of the centers, $(v_{p_1} + v_{p_2})/(v_{n_1} + v_d)$, are shown for various δ-values. At $\delta = 1$, we have a proportional dependence of a_1 on the ratio between the total concentrations of the

centers, and at $\delta > 1$, these dependences do not differ much from linear ones. Note that if the total concentrations of the hole and electron centers are identical, the parameter $a_1 = 1$ for all values of the ratio between the cross-sections of free charge carrier recombination and localization.

It is evident that the number of recombination acts per unit time in the quasi-equilibrium stationary state is equal to the number of electron-hole pairs. Let us determine the relative contribution R of each recombination channel to the total recombination flux through the parameter a_1 and the concentrations of the centers. Using the relation $1 = R_{n_r}^+ + R_{n_1}^+ + R_{p_1}^- + R_{p_2}^-$ and the balance equation $p_1 + p_2 = n_i + n_d$, it is easy to obtain

$$R_{n_r}^+ = \frac{J_{n_r}^+}{G} = \tau^+ u^+ \sigma_{\text{rec}} n_d = \frac{1}{1+a_1} \frac{n_d}{n_d + n_1} =$$
$$= \frac{\nu_d}{(1+a_1)(\nu_d + \nu_{n_1})}, \tag{6a}$$

$$R_{n_1}^+ = \frac{J_{n_1}^+}{G} = \tau^+ u^+ \sigma_{\text{rec}} n_1 = \frac{1}{1+a_1} \frac{n_1}{n_d + n_1} =$$
$$= \frac{\nu_{n_1}}{(1+a_1)(\nu_d + \nu_{n_1})}, \tag{6b}$$

$$R_{p_1}^- = \frac{J_{p_1}^-}{G} = \tau^- u^- \sigma_{\text{rec}} p_1 = \frac{a_1}{1+a_1} \frac{p_1}{p_1 + p_2} =$$
$$= \frac{a_1 \nu_{p_1}}{(1+a_1)(\nu_{p_1} + \nu_{p_2})}, \tag{6c}$$

$$R_{p_2}^- = \frac{J_{p_2}^-}{G} = \tau^- u^- \sigma_{\text{rec}} p_2 = \frac{a_1}{1+a_1} \frac{p_2}{p_1 + p_2} =$$
$$= \frac{a_1 \nu_{p_2}}{(1+a_1)(\nu_{p_1} + \nu_{p_2})}. \tag{6d}$$

Expectedly, the main but not the only factor governing the luminescence intensity of any center is the concentration of this center in the material.

Thus, in the framework of the first model for crystal phosphor, all parameters of stationary luminescence (the center recharging levels, the accumulated light sum, the intensities of luminescence bands) can be obtained if at least the concentration ratio for the centers and the cross-section ratio δ are known for the specimen. However, for real materials, the concentration ratios for various local centers may differ by orders of magnitude, which leads to a large number of possible options. Therefore, let us look for general regularities and tendencies for all possible variants of center concentrations. For example, the ratio between the total recombination fluxes with the
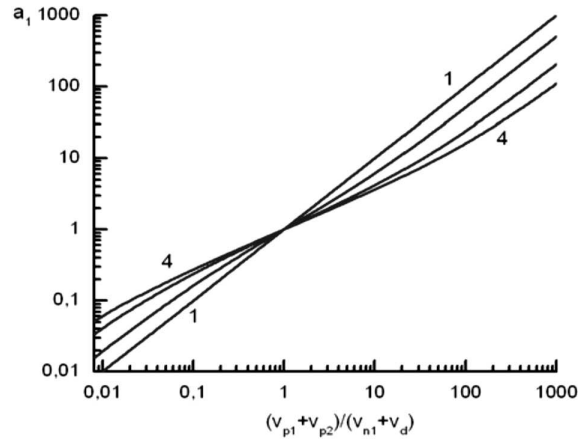
Fig. 7. Dependence of the parameter a_1 on the ratio $(v_{p_1} + v_{p_2})/(v_{n_1} + v_d)$ between the total center concentrations for $\delta = 1$ (*1*), 2 (*2*), 5 (*3*), and 10 (*4*)

electron, $R_{p_1}^- + R_{p_2}^-$, and hole, $R_{n_r}^+ + R_{n_1}^+$, recombination mechanisms is determined by two antibatic functions (6): $a_1/(1+a_1)$ and $1/(1+a_1)$. For the luminescence centers with the same recombination mechanisms, the recombination flux ratio is constant according to Eqs. (3) and (6),

$$\frac{J_{p_1}^-}{J_{p_2}^-} = \frac{p_1}{p_2} = \frac{R_{p_1}^-}{R_{p_2}^-} = \frac{v_{p_1}}{v_{p_2}} = \frac{J_{630}^-}{J_{970}^-}, \tag{7}$$

and is determined only by the ratio between the concentrations of those centers in the temperature interval where no temperature-induced quenching of such centers takes place. Moreover, this ratio does not depend on the number of centers with another recombination mechanism.

For the ratio between the recombination fluxes through centers with opposite recombination mechanisms, we have

$$\frac{J_{p_1}^-}{J_{n_1}^+} = \frac{R_{p_1}^-}{R_{n_1}^+} = a_1 \frac{v_{p_1}}{v_{n_1}} \left(\frac{v_d + v_{n_1}}{v_{p_1} + v_{p_2}} \right) =$$
$$= a_1 \frac{p_1}{n_1} = \frac{v_{p_1}}{v_{n_1}} \left(\frac{a_1 + \delta}{1 + a_1 \delta} \right) = \frac{v_{p_1}}{v_{n_1}} Y_1 = \frac{J_{630}^-}{J_{630}^+}. \tag{8}$$

The plots of the function $Y_1 = (a_1 + \delta)/(1 + a_1 \delta)$ are shown in Fig. 8. One can see that the intensity ratio for the luminescence bands with opposite recombination mechanisms is considerably affected not only by the concentration ratio between the corresponding centers but also by the ratio δ between the recombination and localization cross-sections. The function Y_1 varies from δ to $1/\delta$.

5.2. Model of crystal phosphor with recombination dipole-centers

This model of crystal phosphor differs from the previous one in that instead of two independent luminescence centers with the electron, J_{D}^- (J_{630}^-), and hole, J_{D}^+ (J_{630}^+), recombination mechanisms, we have one dipole-center (D-center) with the concentration v_{D}, at which both alternative recombination mechanisms can be realized.

The same notation for the concentrations and parameters as in the previous model will be used: $a_2 = N^- u^- / P^+ u^+ = \tau^- u^- / \tau^+ u^+$ and $\delta = \sigma_{\mathrm{rec}} / \sigma_{\mathrm{loc}}$. Additionally, the following notations are introduced: n_{D} and p_{D} are the concentrations of localized electrons and holes, respectively, at the D-center, and $f_0 = v_{\mathrm{D}} - n_{\mathrm{D}} - p_{\mathrm{D}}$ is the concentration of uncharged D-centers, at which the initial localization of free electrons or holes can occur.

In the framework of this model, a system of equations similar to Eqs. (2) can be written for the crystal phosphor in the stationary state:

$$\begin{cases} N^- = G\tau^-, \\ P^+ = G\tau^+, \\ 0 = N^- u^- \sigma_{\mathrm{loc}} (v_d - n_d) - P^+ u^+ \sigma_{\mathrm{rec}} n_d, \\ 0 = N^- u^- \sigma_{\mathrm{loc}} f_0 - P^+ u^+ \sigma_{\mathrm{rec}} n_{\mathrm{D}}, \\ 0 = P^+ u^+ \sigma_{\mathrm{loc}} f_0 - N^- u^- \sigma_{\mathrm{rec}} p_{\mathrm{D}}, \\ f_0 + n_{\mathrm{D}} + p_{\mathrm{D}} = v_{\mathrm{D}}, \\ 0 = P^+ u^+ \sigma_{\mathrm{loc}} (v_{p_2} - p_2) - N^- u^- \sigma_{\mathrm{rec}} p_2, \\ n_d + n_{\mathrm{D}} = p_{\mathrm{D}} + p_2 = \Sigma_2. \end{cases} \quad (9)$$

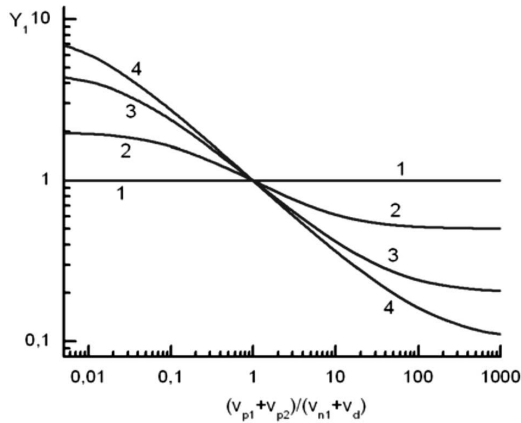For the components of the luminescence band intensity, we can write:

Fig. 8. Dependences of Y_1 on the ratio $(v_{p_1} + v_{p_2})/(v_{n_1} + v_d)$ between the total center concentrations for $\delta = 1$ (*1*), 2 (*2*), 5 (*3*), and 10 (*4*)

• the component

$$J_{n_r}^+ = N^- u^- \sigma_{\mathrm{loc}} (v_d - n_d) = P^+ u^+ \sigma_{\mathrm{rec}} n_d$$

is associated with non-radiative recombination of free holes with trapped electrons;
• the component

$$J_{\mathrm{D}}^+ = N^- u^- \sigma_{\mathrm{loc}} f_0 = P^+ u^+ \sigma_{\mathrm{rec}} n_{\mathrm{D}}$$

is associated with recombination of free holes with electrons localized at the D-center (the hole recombination mechanism);
• the component

$$J_{\mathrm{D}}^- = P^+ u^+ \sigma_{\mathrm{loc}} f_0 = N^- u^- \sigma_{\mathrm{rec}} p_{\mathrm{D}}$$

is associated with recombination of free electrons with holes localized at the D-center (the electron recombination mechanism);
• and the component

$$J_{p_2}^- = P^+ u^+ \sigma_{\mathrm{loc}} (v_{p_2} - p_2) = N^- u^- \sigma_{\mathrm{rec}} p_2$$

is associated with recombination of free electrons with holes localized at the 970-nm center (the electron recombination mechanism).

Accordingly, for the concentrations of localized charge carriers, we obtain

$$\begin{aligned} n_d &= \frac{v_d}{1 + \frac{\delta}{a_2}}, \quad p_2 = \frac{v_{p_2}}{1 + a_2 \delta}, \\ n_{\mathrm{D}} &= \frac{f_0 a_2}{\delta} = \frac{v_{\mathrm{D}} a_2}{\delta \left(1 + \frac{a_2}{\delta} + \frac{1}{a_2 \delta}\right)}, \\ p_{\mathrm{D}} &= \frac{f_0}{a_2 \delta} = \frac{v_{\mathrm{D}}}{1 + a_2^2 + a_2 \delta}, \\ \frac{n_{\mathrm{D}}}{p_{\mathrm{D}}} &= a_2^2, \quad f_0 = \frac{v_{\mathrm{D}}}{1 + \frac{a_2}{\delta} + \frac{1}{a_2 \delta}}. \end{aligned} \quad (10)$$

In this case, $\frac{n_d}{v_d} \neq \frac{n_{\mathrm{D}}}{v_{\mathrm{D}}}$ and $\frac{p_2}{v_{p_2}} \neq \frac{p_{\mathrm{D}}}{v_{\mathrm{D}}}$, i.e., the levels in the centers for filling with charge carriers are different for the carriers of the same sign. But the following equalities hold:

$$\begin{aligned} \frac{n_d}{v_d} &= \frac{n_{\mathrm{D}}}{n_{\mathrm{D}} + f_0} = \frac{n_{\mathrm{D}}}{v_{\mathrm{D}} - p_{\mathrm{D}}} = r_e, \\ \frac{p_2}{v_{p_2}} &= \frac{p_{\mathrm{D}}}{p_{\mathrm{D}} + f_0} = \frac{p_{\mathrm{D}}}{v_{\mathrm{D}} - n_{\mathrm{D}}} = r_h. \end{aligned} \quad (11)$$

That is, the mentioned levels become identical for the carriers of the same sign if the concentration of the
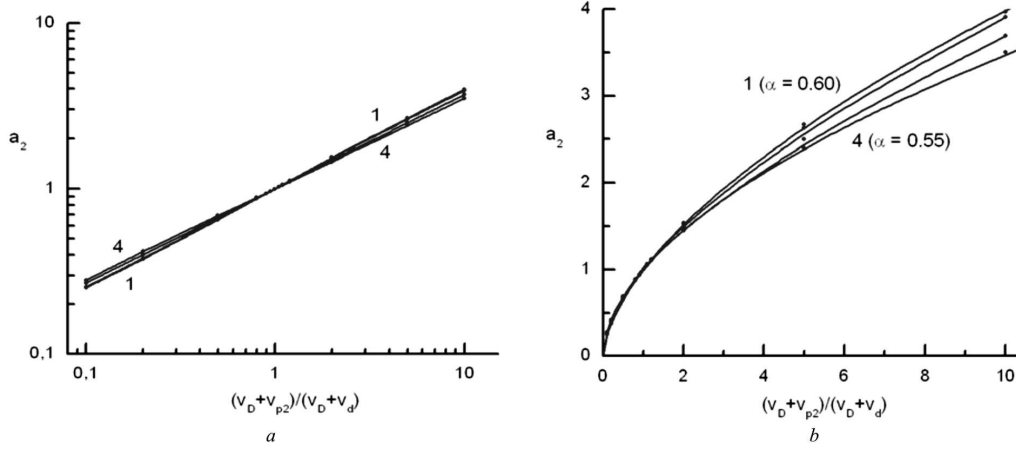
Fig. 9. Values of the parameter $a_2 = N^- u^- / P^+ u^+ = J_\mathrm{D}^+ / J_\mathrm{D}^-$ calculated for various ratios $(v_\mathrm{D} + v_{p_2})/$ $/(v_\mathrm{D} + v_d)$ between the total center concentrations for $\delta = 1$ (*1*), 2 (*2*), 5 (*3*), and 10 (*4*) and plotted in the log-log (*a*) and linear (*b*) scales

centers occupied with the carriers of the opposite sign is excluded from the concentration of D-centers. To determine the parameter a_2 as a function of δ and the concentrations of the centers, dependences (10) obtained for localized charge carriers have to be substituted into the balance equation:

$$\frac{v_d}{1 + \frac{\delta}{a_2}} + \frac{v_\mathrm{D} a_2}{\delta\left(1 + \frac{a_2}{\delta} + \frac{1}{a_2 \delta}\right)} =$$
$$= \frac{v_{p_2}}{1 + a_2 \delta} + \frac{v_\mathrm{D}}{a_2 \delta\left(1 + \frac{a_2}{\delta} + \frac{1}{a_2 \delta}\right)}. \tag{12}$$

After simple algebraic transformations and obvious simplifications, we obtain a quartic equation for a_2,

$$a_2^4 + a_2^3\left(\delta + \frac{1}{\delta}\right) + 2a_2^2\left[1 - \left(\frac{v_\mathrm{D} + v_{p_2}}{v_\mathrm{D} + v_d}\right)\right] -$$
$$- a_2\left(\delta + \frac{1}{\delta}\right)\left(\frac{v_\mathrm{D} + v_{p_2}}{v_\mathrm{D} + v_d}\right) - \left(\frac{v_\mathrm{D} + v_{p_2}}{v_\mathrm{D} + v_d}\right) = 0. \tag{13}$$

An analysis of this equation shows that three of its roots are negative and only one root is positive. Just this root is necessary for a_2 because $a_2 > 0$. Using numerical methods, we obtained the dependences of a_2 on the center concentration ratio $(v_\mathrm{D} + v_{p_2})/(v_\mathrm{D} + v_d)$ for various δ-values. These dependencies are presented by dots in Fig. 9. They can be well approximated by the power-law functions (curves in Fig. 9)

$$a_2 = \left(\frac{v_\mathrm{D} + v_{p_2}}{v_\mathrm{D} + v_d}\right)^\alpha. \tag{14}$$

The power exponent slightly varies from $\alpha = 0.60$ at $\delta = 1$ to $\alpha = 0.55$ at $\delta = 10$.

Hence, for this model, we have appreciably sublinear dependences of a_2 on the center concentration ratio $(v_\mathrm{D} + v_{p_2})/(v_\mathrm{D} + v_d)$ for various δ-values. This circumstance is associated, first of all, with the fact that the D-center can initially localize both electrons and holes, as well as with a reduction of the dynamic range for the ratio between the total concentrations of the centers, $(v_\mathrm{D} + v_{p_2})/(v_\mathrm{D} + v_d)$, since the concentration of D-center enters both its numerator and denominator.

For the relative contributions of the recombination fluxes of the centers, we obtain

$$R_{n_r}^+ = \frac{J_{n_r}^+}{G} = \tau^+ u^+ \sigma_\mathrm{rec} n_d = \frac{1}{1 + a_2}\frac{n_d}{n_d + n_\mathrm{D}} =$$
$$= \frac{1}{1 + a_2}\frac{1}{1 + \frac{v_\mathrm{D}}{v_d}\left(\frac{a_2 + \delta}{a_2 + \delta + 1/a_2}\right)} = \frac{1}{1 + a_2}\frac{1}{1 + \frac{v_\mathrm{D}}{v_d}Y_3}, \tag{15a}$$

$$R_\mathrm{D}^+ = \frac{J_\mathrm{D}^+}{G} = \tau^+ u^+ \sigma_\mathrm{rec} n_\mathrm{D} = \frac{1}{1 + a_2}\frac{n_\mathrm{D}}{n_d + n_\mathrm{D}} =$$
$$= \frac{1}{1 + a_2}\frac{1}{1 + \frac{v_d}{v_\mathrm{D}}\left(\frac{a_2 + \delta + 1/a_2}{a_2 + \delta}\right)} = \frac{1}{1 + a_2}\frac{1}{1 + \frac{v_d}{v_\mathrm{D}}/Y_3}, \tag{15b}$$

$$R_\mathrm{D}^- = \frac{J_\mathrm{D}^-}{G} = \tau^- u^- \sigma_\mathrm{rec} p_\mathrm{D} = \frac{a_2}{1 + a_2}\frac{p_\mathrm{D}}{p_\mathrm{D} + p_2} =$$
$$= \frac{a_2}{1 + a_2}\frac{1}{1 + \frac{v_{p_2}}{v_\mathrm{D}}\left(\frac{1 + a_2\delta + a_2^2}{1 + a_2\delta}\right)} = \frac{a_2}{1 + a_2}\frac{1}{1 + \frac{v_{p_2}}{v_\mathrm{D}}/Y_2}, \tag{15c}$$
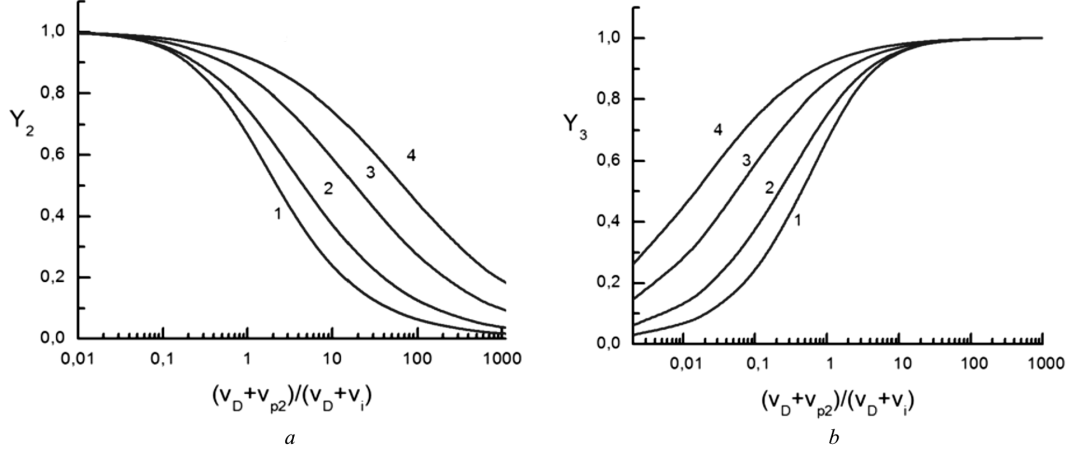
Fig. 10. Dependences of functions Y_2 (*a*) and Y_3 (*b*) on the ratio $(v_D + v_{p_2})/(v_D + v_d)$ between the total center concentrations for $\delta = 1$ (*1*), 2 (*2*), 5 (*3*), and 10 (*4*)

$$R_{p_2}^- = \frac{J_{970}^-}{G} = \tau^- u^- \sigma_{\text{rec}} p_2 = \frac{a_2}{1 + a_2} \frac{p_2}{p_D + p_2} =$$

$$= \frac{a_2}{1 + a_2} \frac{1}{1 + \frac{v_D}{v_{p_2}} \left(\frac{1 + a_2\delta}{1 + a_2\delta + a_2^2} \right)} = \frac{a_2}{1 + a_2} \frac{1}{1 + \frac{v_D}{v_{p_2}} Y_2}. \tag{15d}$$

The introduction of the functions $Y_2 = (1 + a_2\delta)/(1 + a_2\delta + a_2^2)$ and $Y_3 = (a_2 + \delta)/(a_2 + \delta + 1/a_2)$ simplifies the analysis of changes in the intensity of luminescence bands with the variation of center concentrations. As in the previous model, the same two antibatic dependences, $a_2/(1 + a_2)$ and $1/(1 + a_2)$, determine the ratio between the total recombination fluxes according to the electron and hole recombination mechanisms. In this case, the dependences for the ratio between the intensities of the D-center luminescence bands are determined from Eqs. (10):

for the bands with opposite recombination mechanisms,

$$\frac{J_D^+}{J_D^-} = \frac{1}{a_2} \frac{n_D}{p_D} = a_2 = \left(\frac{v_D + v_{p_2}}{v_D + v_d} \right)^{\alpha(\delta)}, \tag{16}$$

and for the bands with the same recombination mechanism,

$$\frac{J_D^-}{J_{p_2}^-} = \frac{p_D}{p_2} = \frac{v_D}{v_{p_2}} \frac{1}{\left(1 + \frac{a_2^2}{1 + a_2\delta}\right)} =$$

$$= \frac{v_D}{v_{p_2}} \left(\frac{1 + a_2\delta}{1 + a_2\delta + a_2^2} \right) = \frac{v_D}{v_{p_2}} Y_2. \tag{17}$$

In Fig. 10, the calculated dependences of Y_2 (*a*) and Y_3 (*b*) on the ratio between the total center concentrations, $(v_D + v_{p_2})/(v_D + v_d)$, are shown for various values of the cross-section ratio δ.

The intensity ratio is substantially affected by the concentrations of all centers. As a result, for the D-center model, the intensity ratios for the luminescence bands with opposite and identical recombination mechanisms were obtained.

Consider the case when only D-centers are available in the crystal and there are no other recombination centers and traps. Then the system of equations (9) can be simplified to the following one:

$$\begin{cases} G = N^- u^- \sigma_{\text{loc}} f_0 + N^- u^- \sigma_{\text{rec}} p, \\ G = P^+ u^+ \sigma_{\text{loc}} f_0 + P^+ u^+ \sigma_{\text{rec}} n, \\ 0 = N^- u^- \sigma_{\text{loc}} f_0 - P^+ u^+ \sigma_{\text{rec}} n, \\ 0 = P^+ u^+ \sigma_{\text{loc}} f_0 - N^- u^- \sigma_{\text{rec}} p_D, \\ n = p, \\ f_0 + n + p = v_D. \end{cases} \tag{18}$$

Its simple solution is

$$\frac{N^-}{P^+} = \frac{u^+}{u^-} = \sqrt{\frac{m_e^*}{m_h^*}}, \quad n = p = \frac{v_D}{2} + \frac{\sigma_{\text{rec}}}{\sigma_{\text{loc}}},$$

$$f_0 = v_D \left(1 - \frac{2}{2 + \sigma_{\text{rec}}/\sigma_{\text{loc}}} \right) = v_D \frac{\sigma_{\text{rec}}/\sigma_{\text{loc}}}{2 + \sigma_{\text{rec}}/\sigma_{\text{loc}}}. \tag{19}$$

For such a crystal, the intensity ratio for the luminescence bands with opposite recombination mechanisms will always be constant, if the internal and external

74

luminescence quenching is neglected):

$$\frac{J^+}{J^-} = \frac{P^+ u^+ \sigma_{\text{rec}} n}{N^- u^- \sigma_{\text{rec}} p} = 1. \tag{20}$$

Hence, for crystal phosphor with only D-centers of recombination, the ratio of electron and hole recombination fluxes is constant.

5.3. Criterion for determining the adequate model

Being different in their nature, the recombination centers in the models concerned do not differ much in the luminescence kinetics. The main difference between those two models manifests itself as different occupation degrees of local centers (traps and recombination centers) depending on the center concentration. If the recombination cross-section is much larger than the localization one ($\delta > 10$), the differences between the respective occupation degrees of both the traps and the recombination centers practically disappear.

To find physical criteria allowing one to decide which model best describes the experimental data, it would be easiest to controllably change the concentrations of the centers. Really, the concentrations of the centers are different in different crystals and it is rather difficult to determine these concentrations with a required accuracy because even their nature is not known for sure. Therefore, a comparison of the luminescence band intensities for various crystals alone will not give the desired result. The variation of the excitation intensity – in practice, this can be done only within one or two orders of magnitude – will also be unsuccessful. As the excitation intensity increases, the concentrations of free carriers (N^- and P^+) grow proportionally, but their ratio does not change. Hence, the parameter a_1 or a_2 will remain unchanged and, therefore, the ratio of band intensities will not vary.

Therefore, in our opinion, the only way is to change the specimen temperature. If the excitation temperature of the specimen is varied from T_1 to T_2 ($T_1 - T_2 = \Delta T > 20$ K), the number of deep traps changes due to the exponential change in the probability of thermal delocalization of charge carriers. In particular, under cooling, some of shallow traps transform into deep ones (Δv_d), which leads to the change of concentration v_d: $v_d(T_2) = v_d(T_1) + \Delta v_d$. Accordingly, the parameter a_1 or a_2 also changes. Using the classical

relationships for the lifetime of free charge carriers, we can write for the first model that

$$a_1 = \frac{N^- u^-}{P^+ u^+} = \frac{G \tau^- u^-}{G \tau^+ u^+} == \frac{u^-}{u^+} \frac{u^+}{u^-} \times$$

$$\times \left[\frac{\sigma_{\text{loc}}(v_{p_1} - p_1) + \sigma_{\text{loc}}(v_{p_2} - p_2) + \sigma_{\text{rec}} n_1 + \sigma_{\text{rec}} n_d}{\sigma_{\text{loc}}(v_d - n_d) + \sigma_{\text{loc}}(v_{n_1} - n_1) + \sigma_{\text{rec}} p_1 + \sigma_{\text{rec}} p_2} \right].$$

The parameter a_1 depends on the temperature because it is determined by the center concentrations and the accumulated light sum. Therefore, as the total concentration of traps increases (v_d), the parameter a_1 decreases according to Eq. (5). But then the magnitude of accumulated light sum will increase. A reduction of the parameter a_1 leads to a change in the occupation degrees of local centers (see Fig. 10, a) and, accordingly, to the variation of relative recombination fluxes. The intensities J_{630} and J_{970} for the first model will decrease identically so that their ratio will remain constant:

$$\left.\frac{J_{p_1}^-}{J_{p_2}^-}\right|_{T_1} = \left.\frac{J_{p_1}^-}{J_{p_2}^-}\right|_{T_2} = \frac{v_{p_1}}{v_{p_2}} = \frac{J_{630}^-}{J_{970}^-}. \tag{21}$$

Simultaneously, the temperature-induced changes of the luminescence bands and their spectral half-widths have to be taken into account. Thus, under cooling from T_1 to T_2, i.e., when the concentration of deep traps for electrons increases, the intensities of luminescence bands with the electron recombination mechanism will decrease identically.

The intensity ratio for the luminescence bands with opposite recombination mechanisms, $J_{\text{D}}^-/J_{\text{D}}^+$, will also remain unchanged:

$$\left.\frac{J_{p_1}^-}{J_{n_1}^+}\right|_{T_1} = a_1(T_1) \frac{v_{p_1}}{v_{n_1}} \frac{v_d + v_{n_1}}{v_{p_1} + v_{p_2}} =$$

$$= \frac{N^- u^-}{P^+ u^+} \frac{v_{p_1}}{v_{n_1}} \frac{v_d + v_{n_1}}{v_{p_1} + v_{p_2}} = \frac{G \tau^- u^-}{G \tau^+ u^+} \frac{v_{p_1}}{v_{n_1}} \frac{v_d + v_{n_1}}{v_{p_1} + v_{p_2}}$$

and, accordingly,

$$\left.\frac{J_{p_1}^-}{J_{n_1}^+}\right|_{T_2} = \frac{v_{p_1} + v_{p_2}}{v_d + \Delta v_d + v_{n_1}} \frac{v_{p_1}}{v_{n_1}} \frac{v_d + \Delta v_d + v_{n_1}}{v_{p_1} + v_{p_2}}. \tag{22}$$

This means that the band intensities $J_{p_1}^-$ (J_{630}^-) and $J_{n_1}^+$ (J_{630}^+) will decrease identically under cooling from T_1 to T_2. A growth of v_d in comparison with v_{n_1} leads, according to Eq. (6), to a reduction of the recombination flux share due to its competition with $J_{n_r}^+$.

From the physical point of view, this result is quite understandable. As the concentration of deep traps for electrons increases, (1) the lifetime of free electrons decreases by a factor of $1 + \Delta v_d/(v_{n_1} + v_d)$, whereas the lifetime of free holes does not change; as a result, (2) the concentration of free electrons decreases identically, and the concentration of free holes does not change; (3) the occupation degree of deep traps for electrons almost does not decrease (as long as their concentration remains much lower than the concentration $(v_{p_1} + v_{p_2})$), but the total concentration of localized electrons increases; (4) the occupation degree of luminescence centers with localized holes also increases almost by a factor of $1 + \Delta v_d/(v_{n_1} + v_d)$; as a result, (5) the intensity of nonradiative recombination increases and the intensities of all luminescence bands slightly decrease; however, (6) the band intensity ratio does not change.

For the second model, let us also compare the change in the intensities of luminescence bands under the material cooling from T_1 to T_2. In this case, some of shallow traps transform into deep ones, which leads to the concentration variation by $(v_d + \Delta v_d)$ and, accordingly, to the reduction of the parameter a_2:

$$a_2 = \frac{N^- u^-}{P^+ u^+} = \frac{G\,\tau^- u^-}{G\,\tau^+ u^+} =$$
$$= \frac{\sigma_{\mathrm{loc}}\,(v_{p_2} - p_2) + \sigma_{\mathrm{loc}} f_0 + \sigma_{\mathrm{rec}} n_{\mathrm{D}} + \sigma_{\mathrm{rec}} n_d}{\sigma_{\mathrm{loc}}\,(v_d - n_d) + \sigma_{\mathrm{loc}} f_0 + \sigma_{\mathrm{rec}} p_{\mathrm{D}} + \sigma_{\mathrm{rec}} p_2}.$$

Note that the ratio between the thermal velocities of electrons and holes does not depend on the temperature and is determined by the effective masses of those particles: $\frac{u^-}{u^+} = \sqrt{\frac{m_h^*}{m_e^*}}$.

For the intensity ratio between the luminescence bands with the same recombination mechanism and in the absence of the luminescence quenching process in the temperature interval from T_1 to T_2, according to Eq. (17), and taking into account that $Y_2(T_1) < Y_2(T_2)$, we obtain

$$\left.\frac{J_{\mathrm{D}}^-}{J_{p_2}^-}\right|_{T_1} = \frac{v_{\mathrm{D}}}{v_{p_2}} \frac{1 + a_2\,(T_1)\,\delta}{1 + a_2\,(T_1)\,\delta + a_2^2\,(T_1)} <$$
$$< \left.\frac{J_{\mathrm{D}}^-}{J_{p_2}^-}\right|_{T_2} = \frac{v_{\mathrm{D}}}{v_{p_2}} \frac{1 + a_2\,(T_2)\,\delta}{1 + a_2\,(T_2)\,\delta + a_2^2\,(T_2)}. \qquad (23)$$

Hence, in contrast to the first model, in the second model, the intensity ratio between the lumines-

cence bands with the same recombination mechanism changes owing to a larger decrease of the intensity J_{970}^-.

According to Eq. (16), for the bands with opposite recombination mechanisms, we obtain

$$\left.\frac{J_{\mathrm{D}}^+}{J_{\mathrm{D}}^-}\right|_{T_1} = a_2(T_1) = \left(\frac{v_{\mathrm{D}} + v_{p_2}}{v_{\mathrm{D}} + v_d}\right)^\alpha >$$
$$> \left.\frac{J_{\mathrm{D}}^+}{J_{\mathrm{D}}^-}\right|_{T_2} = a_2(T_2) = \left(\frac{v_{\mathrm{D}} + v_{p_2}}{v_{\mathrm{D}} + v_d + \Delta v_d}\right)^\alpha. \qquad (24)$$

It is clear that, as was for the first model, the growth of the concentration of deep traps for electrons results in the decrease of the lifetime for free electrons, whereas the lifetime of free holes does not change. However, in this model, it is the ratio between the localized charge carriers of the opposite sign at the D-center, $n_{\mathrm{D}}/p_{\mathrm{D}}$, rather than the occupation degree of the centers that is is decisive for the intensity of luminescence bands. Therefore, the intensity ratio for the luminescence bands will change.

As a result, we obtain that in the case of two independent centers with the electron and hole recombination mechanisms and with constant concentrations, the ratio between the luminescence intensities of those centers **will not change** with the increasing concentrations of deep traps for electrons. At the same time, in the case of dipole-center, the growth in the concentrations of deep traps **will decrease** the luminescence band intensity ratio $J_{\mathrm{D}}^+/J_{\mathrm{D}}^-$.

6. Experimental Values for the Intensity Ratio between the Luminescence Bands

The intensity ratio for the luminescence centers with different recombination mechanisms, J^+/J^-, can be determined experimentally using the criterion obtained in the previous section and the method proposed in work [10]. It is necessary to compare the intensities of phosphorescence and TSL with the intensity of stationary luminescence when various luminescence bands have reached a stationary state. In ZnSe crystals, these are bands at 630 and 970 nm. The indicated data must be supplemented by the data on stationary conductivity and conductivity current relaxation after the excitation termination, as well as by TSC data. All results concerning conductivity must be obtained at the same potential difference applied across the specimen and must correspond to linear sections in the current-voltage characteristics. It

is also important that luminescence in various luminescence bands and conductivity be measured simultaneously, which provides a correct interpretation of the experimental results. The results obtained at two temperatures, $T_1 = 85$ K and $T_2 = 8$ K, should be compared.

First of all, we verified that there was no thermal quenching of luminescence in the temperature interval from 8 to 85 K for both luminescence bands. At both temperatures and under the UV- and X-excitation, the following parameters were determined simultaneously: the stationary intensities of the 630- and 970-nm luminescence bands and the conductivity current; after the excitation termination, the phosphorescence intensities J_{Ph} and the conductivity current relaxation values i_{RC} were determined at the time moments $t_{\mathrm{Ph}} = 50$, 150, and 300 s ($m = 1, 2, 3$); at the further heating, the TSL and TSC intensities were measured: for $T_1 = 85$ K, at temperatures of 110, 130, 150, and 170 K ($k = 1, 2, 3, 4$), and for $T_2 = 8$ K, at temperatures of 25, 30, 40, and 50 K ($k = 1, 2, 3, 4$). Then, the ratios of all those values to the corresponding stationary values were calculated for the 970-nm band and conductivity. Note that the corresponding ratios between the phosphorescence and conductivity current relaxation values are almost indistinguishable. Since phosphorescence, $J_{\mathrm{Ph}}(630)$, and TSL, $J_{\mathrm{TSL}}(630)$, in the 630-nm luminescence band are governed by the electron mechanism of recombination, knowing those ratios, one can determine the intensity of stationary luminescence with the electron mechanism of recombination (J_{630}^-):

$$J_{630}^- = \frac{1}{3}\sum_{m=1}^{3} J_{\mathrm{Ph}-m}(630)\frac{J_{970}^-}{J_{\mathrm{Ph}-m}(970)}, \qquad (25a)$$

$$J_{630}^- = \frac{1}{3}\sum_{m=1}^{3} J_{\mathrm{Ph}-m}(630)\frac{i_{\mathrm{XRC}}}{i_{\mathrm{RC}-m}(970)}, \qquad (25b)$$

$$J_{630}^- = \frac{1}{4}\sum_{k=1}^{4} J_{\mathrm{TSL}-k}(630)\frac{J_{970}^-}{J_{\mathrm{TSL}-k}(970)}, \qquad (25c)$$

$$J_{630}^- = \frac{1}{4}\sum_{k=1}^{4} J_{\mathrm{TSL}-k}(630)\frac{i_{\mathrm{XRC}}}{i_{\mathrm{TSC}-k}}. \qquad (25d)$$

The values obtained for the stationary intensities of the 630-nm band with the electron recombination mechanism allow one to determine the intensity of

the 630-nm band with the hole recombination mechanism ($J_{630}^+ = J_{630} - J_{630}^-$) and their ratio. The corresponding data are given in Table for various specimens under X- and UV-excitation at temperatures of 85 and 8 K. In the last column of the table, the average intensity ratios (J_{630}^+/J_{630}^-) are quoted which were obtained from phosphorescence and TSL.

As expected, the intensity ratios J_{630}^+/J_{630}^- are different in different ZnSe specimens. This is a result of different concentrations of recombination centers and traps in the specimens. But the main thing is that when the temperature decreases from 85 to 8 K and the concentration of deep traps for electrons increases, the ratio J_{630}^+/J_{630}^- decreases as was predicted for the dipole-center. Thus, we can assert that the luminescence center responsible for the wide luminescence band with a maximum at 630 nm is the dipole-center.

Attention is attracted by the experimental fact that the band intensity ratio J_{630}^+/J_{630}^- depends, although not strongly, on the excitation intensity and the external electric field strength. This fact can be explained as follows. In the theoretical consideration, we assumed that the concentration ratio for free charge carriers

$$\frac{N^-}{P^+} = \frac{G\tau^-}{G\tau^+} = \frac{\tau^-}{\tau^+} = \mathrm{const} \neq f(G)$$

does not depend on the excitation intensity and the applied field strength. However, the lux-luminescence

**Experimental values
of the intensity ratio in ZnSe specimens**

ZnSe specimen	Excitation	U_0, V	T_0, K	J^+/J^-
No. 2	$I_X(\max)$	15	85	60–71
	$I_X(\max)$	15	85	65–74
	$I_X(\max)/5$	15	85	41–48
	$I_X(\max)$	6.4	8	22–18
No. 8	$I_X(\max)$	40	85	79–91
	$I_X(\max)$	3.2	8	8.7–6.7
	$I_{UV}(\max)$	15	85	8.4–16
	$I_{UV}(\max)$	3.2	8	25–6
No. 9	$I_X(\max)$	40	85	16–23
	$I_X(\max)$	15	85	27–27
	$I_X(\max)/2.5$	40	85	25–23
	$I_X(\max)/2.5$	15	85	44–29

characteristics (the dependences of luminescence intensity on the excitation intensity) [29] and lux-ampere characteristics [30] experimentally obtained for ZnSe crystals at 85 K reveal a small nonlinear dependence. This means that the excitation intensity has some effect on the concentration ratio between the free charge carriers. Similarly, the experimental current-voltage characteristics of those crystals are also nonlinear [39], and stronger electric fields lead to higher concentrations of free electrons. The nature of all those nonlinearities still remains unknown, so it cannot be taken into account in a theoretical analysis. The influence of free carrier concentrations can also be observed while comparing UV- and X-ray excitations. At UV-excitation, the concentrations of free carriers are higher in the excitation region. Accordingly, we obtain smaller intensity ratios J_{630}^{+}/J_{630}^{-}.

7. Conclusions

The proposed model of dipole-center makes it possible to explain the possibility for the electron and hole recombination mechanisms to be realized at the same luminescence center. The performed theoretical analysis of recombination fluxes and the criterion established for determining the adequate model allowed the authors to assert that the luminescence center responsible for a wide luminescence band with a maximum at 630 nm in ZnSe crystals can be considered as the dipole-center. Furthermore, the parameters of luminescence bands with different recombination mechanisms (the electron, D^{-}, and hole, D^{+}, ones) at room temperature were determined. The results obtained can find practical application because there appear grounds for the technological production of a new type material for high-efficiency scintillation detectors with the dipole-center as the luminescence center.

1. V.I. Gavrilenko, A.M. Grekhov, D.V. Korbutyak, V.G. Litovchenko. *Optical Properties of Semiconductors: A Handbook* (Naukova Dumka, 1987) (in Russian).
2. N.K. Morozova, V.A. Kuznetsov, V.D. Ryzhikov. *Zinc Selenide: Receiving and Optical Properties* (Nauka, 1992) (in Russian).
3. V.E. Lashkarev, A.V. Lyubchenko, M.K. Sheinkman. *Nonequilibrium Processes in Photoconductors* (Naukova Dumka, 1981) (in Russian).
4. L.V. Atroshchenko, S.F. Burachas, L.P. Galchinetskii, B.V. Grinev, V.D. Ryzhikov, N.G. Starzhinskii. *Scintilla-*
tion Crystals and Ionization Radiation Detectors on Their Base (Naukova dumka, 1998) (in Russian).
5. I. Dafinei, M. Fasoli, F. Ferroni *et al.* Low temperature scintillation in ZnSe crystals, *IEEE Trans. Nucl. Sci.* **57**, 1470 (2010).
6. N. Starzhinkiy B. Grinyov, I. Zenya, V. Ryzhikov, L. Gal'chinetskii, V. Silin. New trends in the development of $A^{II}B^{VI}$-based scintillators. *IEEE Trans. Nucl. Sci.* **55**, 1542 (2008).
7. V.D. Ryzhikov *et al.* Properties of semiconductor scintillators ZnSe(Te,O) and integrated scintielectronic radiation detectors based thereon. *IEEE Trans. Nucl. Sci.* **48**, 356 (2001).
8. M.S. Brodyn, V.Ya. Degoda, B.V. Kozhushko, A.O. Sofiienko, V.T. Vesna. Monocrystalline ZnSe as an ionising radiation detector operated over a wide temperature range, *Radiat. Meas.* **65**, 36 (2014).
9. V.Ya. Degoda, A.O. Sofiienko. Effect of traps on current impulse from X-ray induced conductivity in wide-gap semiconductors. *Physica B* **426**, 24 (2013).
10. V.Ya. Degoda, N.Yu. Pavlova, G.P. Podust, A.O. Sofiienko. Spectral structure of the X-ray stimulated phosphorescence of monocrystalline ZnSe. *Physica B* **465**, 1 (2015).
11. M. Alizadeh, V.Ya. Degoda, B.V. Kozhushko, N.Y. Pavlova. Luminescence of dipole-centers in ZnSe crystals. *Funct. Mater.* **24**, 206 (2017).
12. U. Kuhn, F. Lüty. Paraelectric behavior of OH⁻-dipole centers in KCl crystals, *Solid State Commun.* **2**, 281 (1964).
13. U. Kuhn, F. Lüty. Paraelectric behavior of OH⁻-dipole centers in KCl crystals. *Solid State Commun.* **88**, 897 (1993).
14. A.K. Kadashchuk, N.I. Ostapenko, Yu.A. Skryshevskii, V.I. Sugakov, T.O. Susokolova. Clusters of dipole charge-carrier capture centers in organic crystals. *Mol. Cryst. Liq. Cryst.* **201**, 167 (1991).
15. B.S.H. Royce, S. Mascarenhas. Dipole centers and optical absorption in $CaF_2:Ce^{3+}$. *Phys. Rev. Lett.* **27**, 970 (1971).
16. R.A. Maier, T.A. Pomorski, P.M. Lenahan, C.A. Randall. Acceptor-oxygen vacancy defect dipoles and fully coordinated defect centers in a ferroelectric perovskite lattice: Electron paramagnetic resonance analysis of Mn^{2+} in single crystal $BaTiO_3$. *J. Appl. Phys.* **118**, 164102 (2015).
17. R. Baltramiejunas, V.D. Ryzhikov, V. Gavryushin, A. Kazlauskas, G. Raciukaitis, V.I. Silin, D. Juodzbalis, V. Stepankevicius. Luminescent and nonlinear spectroscopy of recombination centers in isovalent doped ZnSe : Te crystals. *J. Luminesc.* **52**, 71 (1992).
18. U. Philipose, S. Yang, T. Xu, H.E. Ruda. Origin of the red luminescence band in photoluminescence spectra of ZnSe nanowires. *Appl. Phys. Lett.* **90**, 063103 (2007).
19. V. Ryzhikov, B. Grinyov, S. Galkin, N. Starzhinskiy, I. Rybalka. Growing technology and luminescent characteristics of ZnSe doped crystals. *J. Cryst. Growth* **364**, 111 (2013).
20. K. Katrunov, V. Ryzhikov, V. Gavrilyuk, S. Naydenov, O. Lysetska, V. Litichevskyi. Optimum design calculations

for detectors based on ZnSe(Te, O) scintillators. *Nucl. Instrum. Methods A* **712**, 126 (2013).

21. V.M. Koshkin, A.Ya. Dulfan, V.D. Ryzhikov, L.P. Gal'chinetskii, N.G. Starzhinskiyet. Thermodynamics of isovalent tellurium substitution for selenium in ZnSe semiconductors. *Funct. Mater.* **8**, 708 (2001).

22. L.V. Atroschenko, L.P. Gal'chinetskii, S.N. Galkin *et al.* Structure defects and phase transition in telluriumdoped ZnSe crystals. *J. Cryst. Growth* **197**, 475 (1999).

23. Woo Gyo Lee, Yong Kyun Kim, Jong Kyung Kim, N. Starzhinskiy, V. Ryzhikov, B. Grinyov. Properties of ZnSe:Te,O crystals grown by Bridgman-Stockbarger method. *J. Nucl. Sci. Technol.* **45**, 579 (2008).

24. J. Mickevicius, G. Tamulaitis, P. Vitta, A. Zukauskas, N. Starzhinskiy, V. Ryzhikov. Characterization of ZnSe(Te) scintillators by frequency domain luminescence lifetime measurements. *Nucl. Instrum. Methods A* **610**, 321 (2009).

25. M. Alizadeh, V.Ya. Degoda. The spectra of X-ray and photoluminescence of high-resistance crystals of ZnSe. *Ukr. J. Phys.* **63**, 557 (2018).

26. M.V. Fok. *Separation of Complex Spectra into Individual Bands Using the Generalized Alentsev Method* (Trudy FIAN SSSR, 1972) (in Russian).

27. M.S. Brodyn, V.Ya. Degoda, N.Yu. Pavlova, G.P. Podust, Ya.P. Kogut, M. Alizadeh, B.V. Kozhushko. The components of 630-nm band in ZnSe and their recombination mechanisms, *Optik* **208**, 164139 (2020).

28. A.F. Lubchenko. *Quantum Transitions in Impurity Centers of Solids* (Naukova Dumka, 1978) (in Russian).

29. V.Ya. Degoda, M. Alizadeh, N.O. Kovalenko, N.Yu. Pavlova. The dependencies of X-ray conductivity and X-ray luminescence of ZnSe crystals on the excitation intensity. *Adv. Condens. Matter Phys.* **2018**, 1515978 (2018).

30. V.Ya. Degoda, M. Alizadeh, Ya.P. Kogut, N.Yu. Pavlova, S.V. Sulima. The influence of UV excitation intensity on photoconductivity and photoluminescence in ZnSe monocrystals. *J. Luminesc.* **205**, 540 (2019).

31. M.V. Fok. *Introduction to Luminescence Kinetics of Crystallophosphors* (Nauka, 1964) (in Russian).

32. V.V. Antonov-Romanovskii. *Photoluminescence Kinetics of Crystallophosphors* (Nauka, 1966) (in Russian).

33. R.H. Bube. *Photoconductivity of Solids* (John Wiley and Sons, 1960).

34. A. Rose. *Concepts in Photoconductivity and Allied Problems* (Interscience Publishers, 1963).

35. S.M. Ryvkin. *Photoelectric Effects in Semiconductors* (Consultants Bureau, 1964).

36. V.Ya. Degoda, A.F. Gumenyuk, Yu.A. Marazuev. *Kinetics of Recombination Luminescence and Conductivity of Crystallophosphors* (Kyiv Nat. Univ. Publ. House, 2016) (in Ukrainian).

37. V.Ya. Degoda, M. Alizadeh. Parameters of charge carrier traps in ZnSe. *Ukr. J. Phys.* **64**, 300 (2019).

38. M. Alizadeh, V.Y. Degoda, G.P. Podust, N.Y. Pavlova. Observation of the kinetic buildup of x-ray conduction current in ZnSe crystals. *J. Appl. Phys.* **128**, 015702 (2020).

39. V.Ya. Degoda, M. Alizadeh, N.O. Kovalenko, N.Yu. Pavlova V-I characteristics of X-ray conductivity and UV photoconductivity of ZnSe crystals, *J. Appl. Phys.* **123**, 075702 (2018).

В.Я. Дегода, М.С. Бродін, М Алізаде,
Г.П. Подуст, Н.Ю. Павлова, Б.В. Кожушко

DIPOLE-ЦЕНТР У КРИСТАЛАХ СЕЛЕНІДУ ЦИНКУ

Встановлено, що відома смуга свічення з максимумом біля 630 нм в нелегованих кристалах ZnSe зумовлена рекомбінацією як вільних електронів на локалізованих дірках, так і рекомбінацією вільних дірок на локалізованих електронах. Такий результат вдалося отримати завдяки порівнянню між собою, по-перше, експериментальних значень стаціонарних інтенсивностей люмінесценції зі значеннями інтенсивностей фосфоресценції та термостимульованої люмінесценції, і, по-друге, величин провідності при стаціонарних умовах з кривими релаксації струму та термостимульованої провідності. Для пояснення нетипових спектральних особливостей смуги свічення 630 нм, запропоновано існування комплексного (не точкового) центра, на якому можуть альтернативно реалізовуватись обидва механізми рекомбінації. Такий центр можна назвати Dipole-центром. Для багатоцентрової моделі кристалофосфору з присутнім у ньому Dipole-центром рекомбінації проведено теоретичний аналіз і встановлено, що саме цей центр зумовлює широку смугу свічення із загальним максимумом при 630 нм. Це дозволяє запропонувати сцинтиляційний матеріал нового типу – з Dipole-центром у ролі центра свічення, який не потребує пасток для забезпечення високого виходу люмінесценції.

Ключові слова: ZnSe, центри свічення у кристалофосфорах, люмінесценція, Dipole-центр.